CHARACTERIZATION OF Ar-DEGASSING FROM ANTARCTIC METEORITES

Ichiro KANEOKA

Geophysical Institute, Faculty of Science, University of Tokyo, 11-16, Yayoi 2-chome, Bunkyo-ku, Tokyo 113

Abstract: Based on the Ar-degassing patterns from the Antarctic meteorites, it is intended to find some relationships between the types of Ar-degassing and the states of Antarctic meteorites.

For this purpose, diffusion parameters (D/a^2, E) were obtained for each meteorite by using the ^{39}Ar-degassing pattern which had been obtained when those meteorites had been dated by the ^{40}Ar-^{39}Ar method. The diffusion constants (D/a^2) are estimated to be $(0.2\text{–}3)\times10^{-5}$ s^{-1} at 1000°C. The activation energies (E) range from about 10 to 50 kcal/mole, but mostly 20 to 40 kcal/mole. Non-equilibrated chondrites seem to have lower activation energies than equilibrated chondrites.

On the basis of integrated fraction of Ar, a diagram is exploited to compare relative degassing patterns of Ar between neutron induced K-derived ^{39}Ar and the others (^{36}Ar, ^{37}Ar, ^{40}Ar). According to the Ar-degassing patterns in this diagram, the Antarctic meteorites are classified into three Types, A, B and C. It is found that achondrites are generally classified into Type A, where ^{40}Ar correlates well with ^{39}Ar and ^{36}Ar (and ^{37}Ar) degass at slightly higher temperatures than ^{39}Ar. Chondrites are classified into Type B, where ^{40}Ar correlates with ^{39}Ar, but ^{36}Ar (and ^{37}Ar) degass at definitely higher temperatures than ^{39}Ar. Weathered achondrites and chondrites are generally grouped into Type C, where ^{40}Ar does not correlate with ^{39}Ar and degassing patterns of ^{36}Ar and ^{37}Ar are also non-systematic. Thus, such classification would give another measure to evaluate the reliability of an ^{40}Ar-^{39}Ar age obtained in addition to conventional criteria.

1. Introduction

Through the investigation of ^{40}Ar-^{39}Ar ages on the Antarctic metorites, it has been found that Ar-degassing characteristics are often disturbed due to weathering of meteorites (*e.g.*, KANEOKA, 1983a, b). To get reliable information on ages, it is essential to evaluate such effects properly.

In our previous papers (KANEOKA, 1980, 1981; KANEOKA *et al.*, 1979), we got ^{40}Ar-^{39}Ar ages on the Antarctic meteorites by applying stepwise heating. If there are some systematic changes in Ar-degassing due to the weathering of a sample, they should also be reflected in the results of the stepwise heating. The degree of degassing rate from a meteorite gives us some information on the diffusion characteristics of Ar through the meteorite. Furthermore, each Ar isotope degasses in different rates at each temperature. By the combination of such information, it may be possible to classify the samples into a few groups, on which the criteria to determine the degree of reliability of the obtained ^{40}Ar-^{39}Ar ages would be settled.

In this study, activation energies for Ar diffusion through each meteorite, whose

^{40}Ar-^{39}Ar age was obtained, have been estimated. Further, degassing patterns of each Ar isotope are compared and classified into three types, by which some secondary effects on ^{40}Ar-^{39}Ar ages might be evaluated. Their relationships with the type of meteorites are also examined to characterize each meteorite from the point of view of Ar-degassing.

2. Diffusion Characteristics

In order to clarify the degassing characteristics of Ar from a meteorite, it is useful to know the parameters of diffusion for each meteorite. Diffusion coefficient D can be expressed in a form,

$$D=D_0 \exp(-E/RT), \tag{1}$$

where E is the activation energy; R: the gas constant; T: the absolute temperature; D_0: a characteristic constant. Practically it is more convenient to use the following form.

$$D/a^2=D_0/a^2 \exp(-E/RT), \tag{2}$$

where "a" indicates a characteristic size of a sample (*e.g.*, the radius in the case of a sphere). If we can estimate D or D/a^2 at each temperature T, the Arrhenius plot ln D (or ln (D/a^2)) *vs.* ln $(1/T)$ would give a straight line with a gradient $(-E/R)$. Thus, we can get a value of E by drawing an Arrhenius plot following a formula of either (1) or (2).

For 14 Antarctic meteorites, ^{40}Ar-^{39}Ar ages were obtained by applying stepwise heating. Hence, if the total concentration of argon is known for a sample, the diffusion coefficient can be calculated from the heating time "t" and the corresponding fractional loss F (FECHTIG and KALBITZER, 1966). In this case, it is necessary to assume a geometry of each grain together with the initial distribution of Ar in the grain. Furthermore, to know the value of diffusion coefficient D, we need to know the characteristic grain size. However, no precise measurements on grain sizes nor geometry were performed for the Antarctic meteorites which were used for ^{40}Ar-^{39}Ar dating. Hence, it is more appropriate in the present study to use the value D/a^2 instead of D to estimate an activation energy E for each meteorite. In the present study, we have intended to get only a general figure concerning the diffusion characteristics of Ar in the Antarctic meteorites and not intended to determine precise values about diffusion parameters. Hence, here we consider a very simple model that each Antarctic meteorite is composed of a sphere with a radius of "a" and a homogeneous distribution of Ar at time zero. No grain size effects are considered.

Based on such a model, the value D/a^2 for Ar at each temperature can be calculated from the data which were used to get ^{40}Ar-^{39}Ar ages of an Antarctic meteorite for each temperature step. An example is shown in Fig. 1. In this Arrhenius plot, the data for ^{40}Ar and ^{39}Ar lie on almost the same straight line and those for ^{37}Ar and ^{36}Ar on another straight line. These straight lines show almost the same gradient, corresponding to an activation energy of about 23 kcal/mole. This means that ^{40}Ar and ^{39}Ar degass very similarly for this sample. ^{37}Ar and ^{36}Ar also degass in a similar manner. However, the former two degass slightly faster than the latter two. In the present study, the main concern about the transportation of Ar is related to that of the radiogenic ^{40}Ar. In

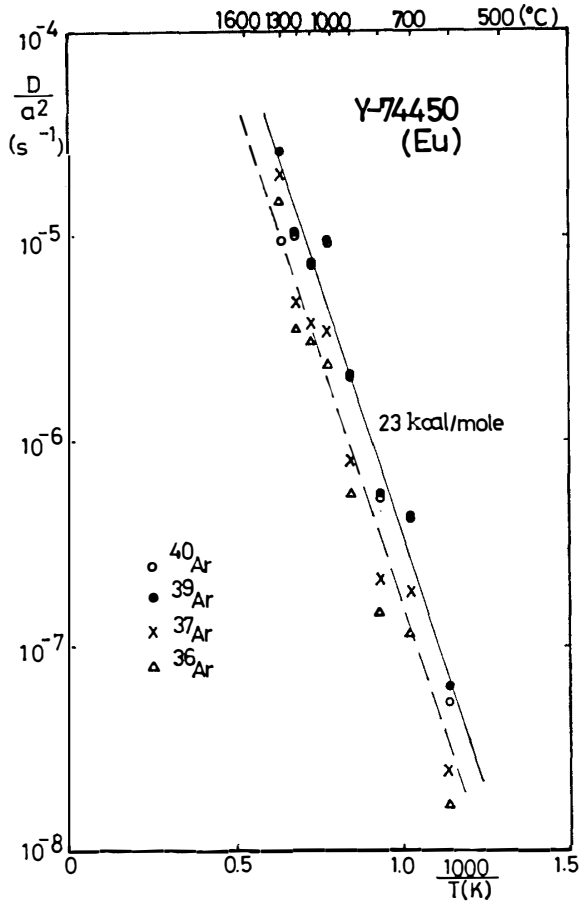

Fig. 1. Arrhenius plot for the sample Y-74450 (eucrite). The solid straight line is drawn for the data of ^{40}Ar and ^{39}Ar, and the dotted line for the data of ^{37}Ar and ^{36}Ar. Note that both lines show the same gradient, indicating an activation energy of 23 kcal/mole.

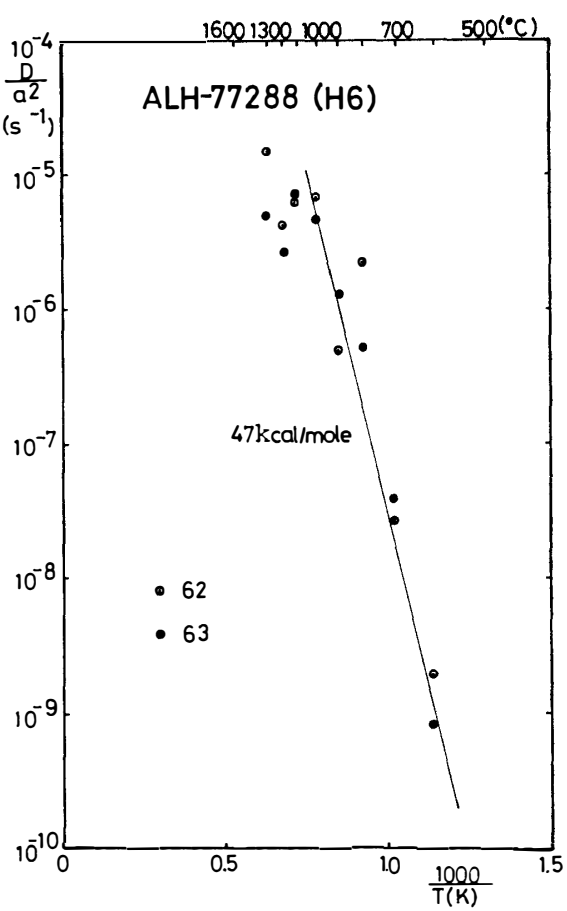

Fig. 2. Arrhenius plot for the sample ALH-77288 (H6). The samples ALH-77288,62 and ALH-77288,63 were taken from different portions of the same block of the meteorite. For detailed sample description, refer to KANEOKA (1983b).

natural samples, however, the radiogenic ^{40}Ar might have been disturbed already to some extent. Hence to get an idea about the characteristics of Ar movement, it is better to use neutron-induced ^{39}Ar as an indicator. Hence, diffusion parameters were obtained for only ^{39}Ar for the other meteorites and we assume them to represent the characteristics of Ar movement in an Antarctic meteorite.

Figure 2 indicates an example where two portions of a meteorite show almost similar characteristics in the Arrhenius plot. The portion 62 represents the outer surface and the portion 63 the inner part of the meteorite ALH-77288 (KANEOKA, 1983b). The data for temperature fractions of less than 1000°C lie roughly on a straight line in the Arrhenius plot, indicating an activation energy of almost 47 kcal/mole. However, the data for fractions of more than 1000°C scatter, which would correspond to some disturbances in the structure of the sample. In such a case, activation energy cannot be estimated for these temperature fractions.

In Fig. 3, another example is shown. For this sample, two kinds of activation

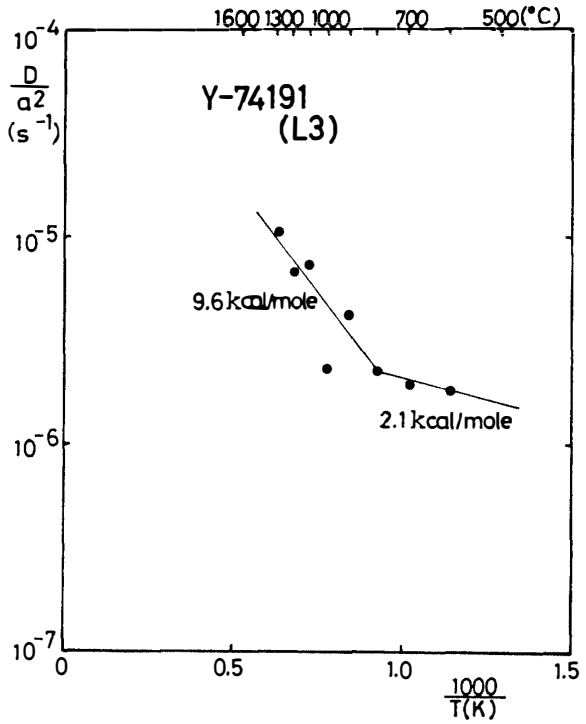

Fig. 3. Arrhenius plot for the sample Y-74191 (L3). Note the difference in the gradient of the line below 800°C and above that temperature.

Table 1. Diffusion parameters for Antarctic meteorites.

Meteorite	Class	$(D/a^2)_{1000°C}$* (s^{-1}) × 10^{-5}	E (kcal/mole)	Temperature** range (°C)
Chondrite				
Y-74640	H6	0.21	26	700–1350
ALH-77288,62	H6	0.50	47	600–1000
63	H6			
Y-74191	L3	0.47	(2.1)	600– 800
			9.6	800–1300
ALH-77015	L3	(0.52)	(21)	700–1000
			49	1100–1450
Y-74190	L6	2.1	30	600–1000
ALH-761,61	L6	1.9	36	
62	L6	2.5	44	600–1000
64	L6	2.8	38	
ALH-77214	L or LL	(1.3)	37	700– 900
ALH-77304	LL3	0.78	17	700–1450
Y-75258	LL6	1.7	33	600–1000
Achondrite				
Y-74159	Eucrite	0.81	25	600–1150
Y-74450	Eucrite	0.43	23	600–1300
ALH-765	Eucrite	1.6	32	600–1000
Y-7308	Howardite	0.75	7.5	700–1000
			20	1000–1450
Y-74097	Diogenite	0.39	26	700–1350

*The value in parentheses is less reliable than the others.
**Activation energy (E) for each meteorite was estimated from the data for these temperatures.

energies seem to be defined for lower and higher temperatures, respectively, though the former is less reliable than the latter. The data for fractions of less than 800°C give an activation energy of about 2.1 kcal/mole, whereas those for fractions of more than 800°C indicate an activation energy of about 9.6 kcal/mole. It is expected that such a change may correspond to that of structures of degassing portions in the sample.

Considering those factors stated above, the estimated diffusion parameters for the Antarctic meteorites are summarized in Table 1. As stated before, these values are calculated based on a very simple model resulting in involvement of many uncertainties. Hence, they should be regarded to show only rough measures about the diffusion characteristics Ar for the Antarctic meteorites whose ^{40}Ar-^{39}Ar ages were obtained previously. From this table, it is pointed out that these Antarctic meteorites show activation energies in the range of about 10–50 kcal/mole, but mostly 20–40 kcal/mole. No clear relationships are observed between the value of activation energy and the group of meteorite, though achondrites seem to show rather similar values of activation energies.

In Fig. 4, values of activation energies of the Antarctic meteorites which were ob-

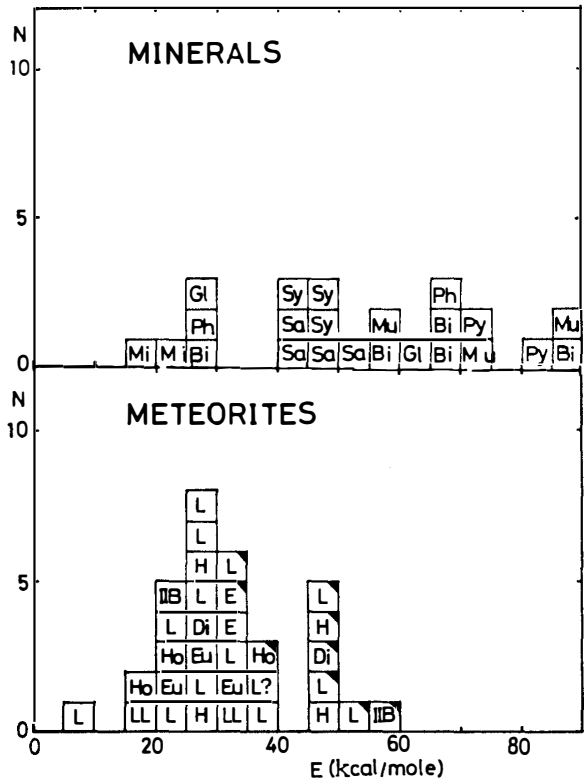

Fig. 4. Summaries of activation energies obtained for the Antarctic meteorites in the present study and those reported for other meteorites and minerals separated from terrestrial rocks.
For meteorites, those designated by black triangles at the upper right corners are corrected for grain size effect, but others are not. Data sources: FECHTIG and KALBITZER (Table 5, 104–105, 1966) and the present study.
Bi: Biotite, Mu: Muscovite, Ph: Phlogopite, Gl: Glauconite, Mi: Microcline, Sa: Sanidine, Sy: Sylvite, Py: Pyroxene.
L: L-chondrite, H: H-chondrite, LL: LL-chondrite, Eu: Eucrite, Ho: Howardite, Di: Diogenite, IIB: IIB-iron meteorite.

tained in this study are compared with those reported for other meteorites. Furthermore, they are compared with those of minerals separated from terrestrial samples. For meteoritic samples, higher activation energies up to about 69 kcal/mole are reported. However, much higher values are observed in minerals. Meteorite samples are composites of a number of different minerals. In such a complex system, averaged diffusion parameters (E, D/a^2) might include both the effect of non-volume diffusion and that of volume diffusion. It is expected that in an ideal case they can be separated by showing different straight lines with different gradients for lower and higher temperatures (FECHTIG and KALBITZER, 1966). The case of the sample Y-74191 may be such an example as shown in Fig. 3. However, the effect of non-volume diffusion might be mostly included in the lowest temperature fraction in the present case, because its degassing temperature reaches up to 600 or 700°C which is relatively high compared with the applied temperature in a typical diffusion experiment (*e.g.* FECHTIG and KALBITZER, 1966).

As stated before, the present study does not include the correction for grain size effect, which might result in lower activation energies than those corrected for this effect (FECHTIG and KALBITZER, 1966). The difference in the apparent activation energies between the present results and the reported ones might be at least partly due to this effect. As long as the same condition is applied, however, the comparison of diffusion parameters among the Antarctic meteorites would be useful practically. The present discussions concerning diffusion parameters are based on this belief.

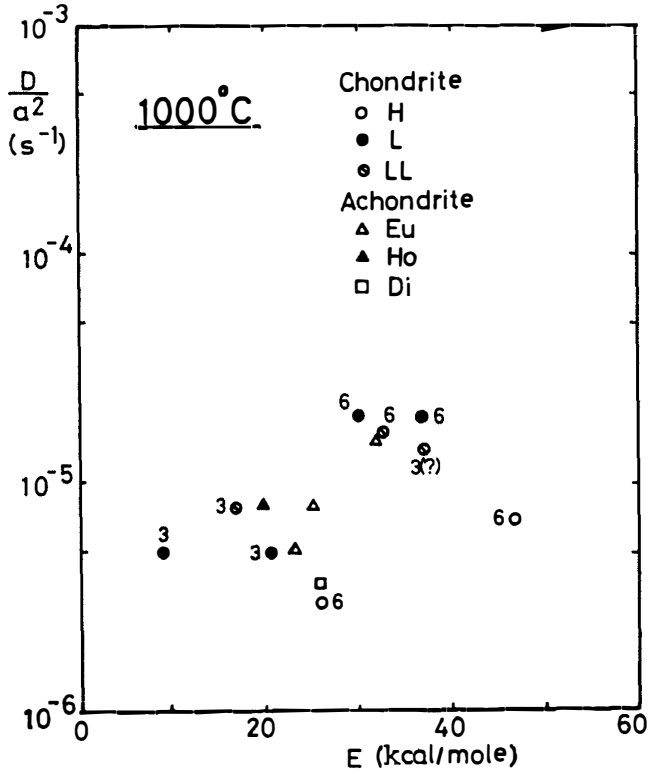

Fig. 5. The diffusion constant $(D/a^2)_{1000°C}$ vs. activation energy (E). The numerical figure at the side of each symbol indicates the degree of equilibrium for chondrite defined by VAN SCHMUS and WOOD (1967).

In Fig. 5, diffusion constant D/a^2 at 1000°C is plotted against the activation energy (E) for the Antarctic meteorite. The choice of the temperature 1000°C is rather arbitrary. However, at this temperature, we can safely say that the effect of volume diffusion would be essential and K-including minerals already degass radiogenic ^{40}Ar largely by this temperature. In this figure, we can roughly assign two groups. The one has a higher $(D/a^2)_{1000°C}$ value together with a higher activation energy (E) compared with another group. Four among five achondrites studied here belong to the latter group. Hence, achondrites may have relatively similar diffusion characteristics compared with those of chondrites. Apparently, no systematics seem to exist for the chondrite samples in Fig. 5. It is interesting to note, however, that chondrites with higher $(D/a^2)_{1000°C}$ and E are mostly equilibrated ones and those with lower $(D/a^2)_{1000°C}$ and E are mostly non-equilibrated ones. This means that the characteristics concerning diffusion parameters of the Antarctic meteorites might reflect the state of each mineral and their complexes, but are not always controlled by chemical compositions of meteorites. Since the number of investigated cases is limited, it may be premature to deduce this conclusion as a general one. However, it is worth trying to examine this point further in order to clarify the characteristics of Ar-degassing from the Antarctic meteorites. Furthermore, we found no apparent relationships between the values of diffusion parameters and the degree of weathering, the effect of which can be clarified in the Ar-release patterns as shown in the next section.

From the present results, it is inferred that the diffusion constants (D/a^2) for most meteorites are in the order of 10^{-5}–10^{-4} s^{-1} at around 1000–1300°C. These numbers give us some measures for the necessary time to degass Ar from these meteorites. Simple calculation suggests that Ar can diffuse out almost completely from these meteorites within a few hours to one day if such temperatures are maintained. If the temperatures are around 700–800°C, the diffusion constants D/a^2 decrease down to 10^{-8}–10^{-6} s^{-1}, which are more variable among meteorites compared with those at higher temperatures. Under such conditions, the required period to degass Ar from these meteorites increases up to more than 10 days to nearly 3 years. To degass Ar almost completely from meteoritic materials, it is necessary to maintain relatively high temperatures for a relatively long time. Hence, in the case of collision between meteoritic materials, the degassing of Ar should have occurred not only at the instant of collision but also at the later period during which relatively high temperatures were kept for some time. However, more detailed studies are necessary to infer the degassing history of each meteorite.

3. Types of Ar-degassing

In order to clarify the characteristics of Ar-degassing from the Antarctic meteorites, a diagram which shows a fraction of released Ar to the total one against a temperature is often used (*e.g.*, KANEOKA, 1981). In such a diagram, it is useful to find detailed structures of degassing patterns for Ar in a sample. To generalize the degassing patterns of Ar, however, such expressions include too many complexities. For this purpose, it is more convenient to use a diagram where the integrated fraction of Ar is shown against the degassing temperature. An example is shown for the sample Y-74450 (Eu) in Fig. 6.

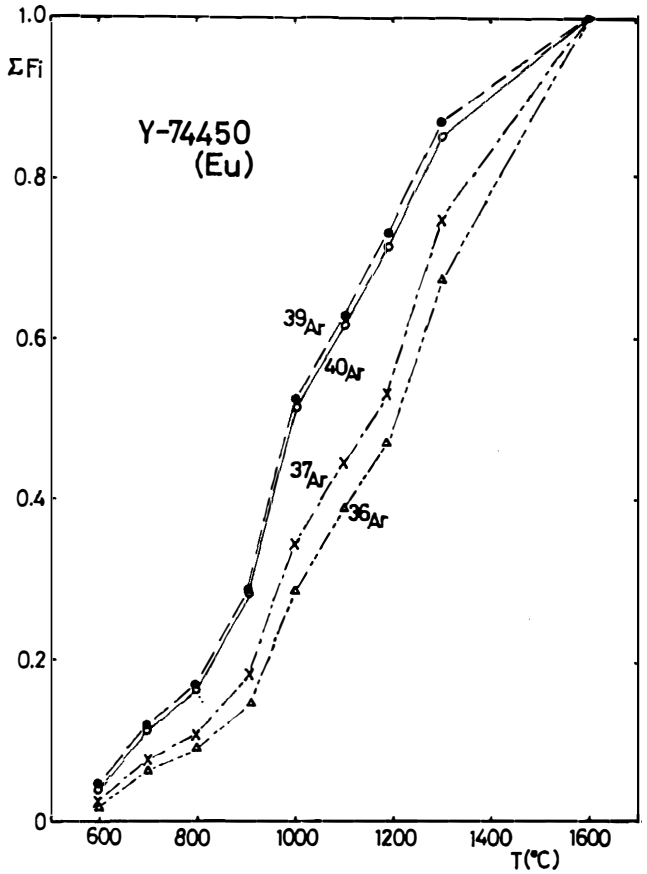

Fig. 6. The integrated fraction of Ar (ΣFi) vs. degassing temperature for the sample Y-74450 (eucrite).

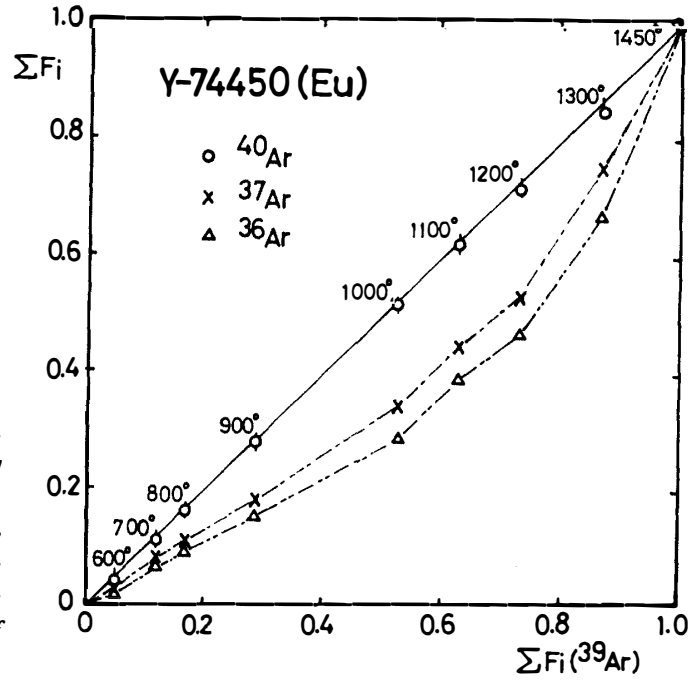

Fig. 7. The integrated fraction of Ar (^{36}Ar, ^{37}Ar, ^{40}Ar) vs. the integrated fraction of ^{39}Ar for the sample Y-74450. The numerical figures plotted on a line with a gradient of 45° indicate degassing temperatures. When no secondary ^{40}Ar loss occurred, the integrated fraction of ^{40}Ar should lie on this straight line.

In Fig. 6, the ordinate indicates the integrated fraction of Ar to the total one and the abscissa the degassing temperature. ^{39}Ar and ^{37}Ar are K- and Ca-derived isotopes induced by neutron irradiation, respectively. In this figure, the degassing temperature is an important factor to form this diagram. However to generalize the degassing pattern of Ar, we do not always need the value of temperature as long as we discuss the difference in the release patterns of each Ar isotope. Furthermore, the measurement of temperature includes some uncertainties. Hence, another presentation is shown for the same sample in Fig. 7.

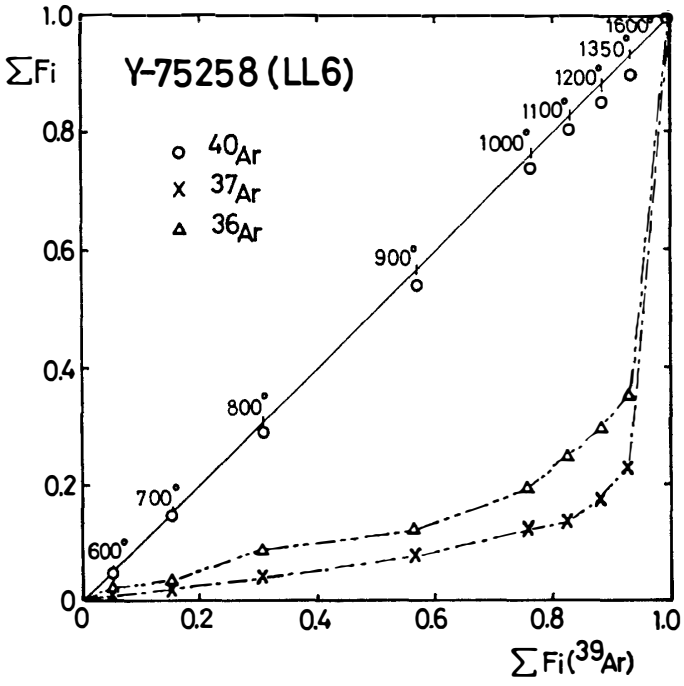

Fig. 8. The integrated fraction of Ar (^{36}Ar, ^{37}Ar, ^{40}Ar) vs. the integrated fraction of ^{39}Ar for the sample Y-75258 (LL6).

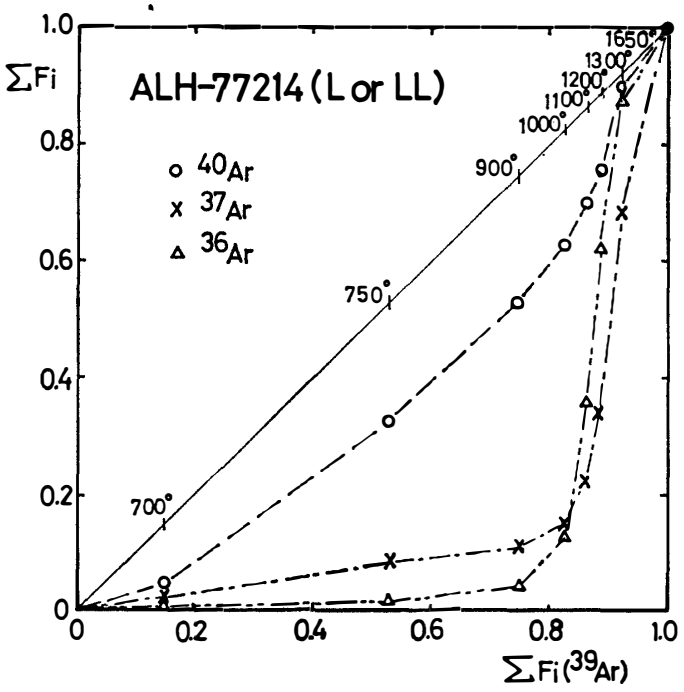

Fig. 9. The integrated fraction of Ar (^{36}Ar, ^{37}Ar, ^{40}Ar) vs. the integrated fraction of ^{39}Ar for the sample ALH-77214 (L or LL).

In Fig. 7, the integrated fraction of Ar (^{36}Ar, ^{37}Ar, ^{40}Ar) to the total one is shown against the integrated fraction of ^{39}Ar to the total ^{39}Ar. In this figure, the uncertainties in the temperature measurement do not affect the pattern at all. Furthermore, the similarities in the release patterns between ^{39}Ar and ^{40}Ar indicate that the plots for ^{40}Ar almost lie on a straight line with a gradient of 45°. Hence we can evaluate the similarities of release patterns much more easily in this figure compared with those as shown in Fig. 6. The release patterns for ^{36}Ar and ^{37}Ar show downward-convex curves, suggesting the difference in the degassing degrees compared with ^{39}Ar.

In Figs. 8 and 9, the other two examples are shown in the same plots. In the case of the sample Y-75258 (Fig. 8), the pattern for ^{40}Ar is almost the same as that for the sample Y-74450. However, the difference in the integrated released fraction is much larger for ^{36}Ar and ^{37}Ar at the intermediate integrated fraction for ^{39}Ar. This means that ^{36}Ar and ^{37}Ar degass at much higher temperatures compared with ^{39}Ar and ^{40}Ar for this sample.

In the case of the sample ALH-77214 (Fig. 9), the data for ^{40}Ar do not lie on the straight line with a gradient of 45°. Furthermore, the lines for ^{36}Ar and ^{37}Ar cross each other, showing some complexities in the released patterns for these Ar isotopes. This sample is apparently weathered (KANEOKA, 1980) and such effect is clearly observed in this figure.

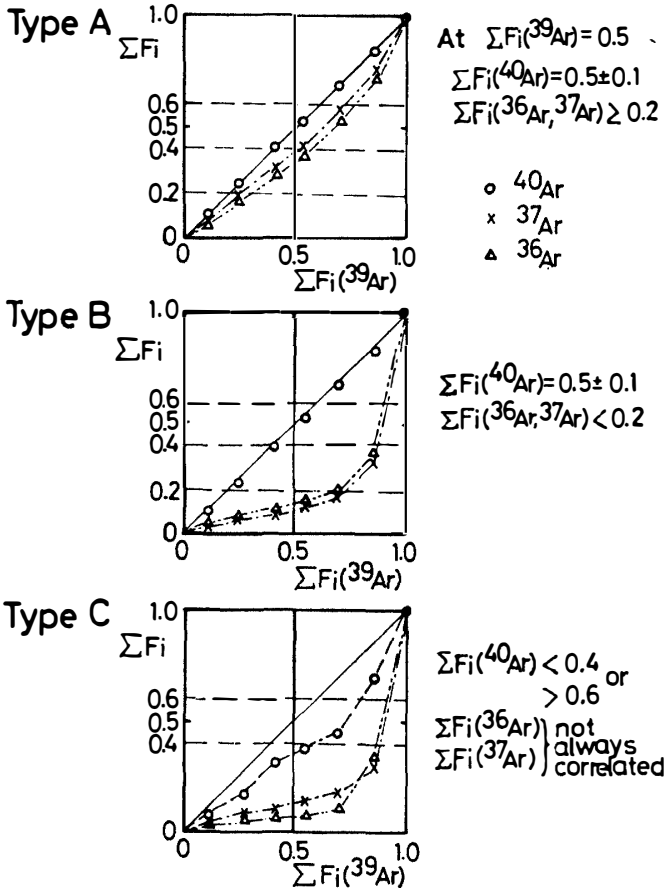

Fig. 10. Classification of Ar-degassing type. Schematic figures for each type are shown.

By using such a diagram, classification of degassing type of Ar from the Antarctic meteorite is made. To classify the type, it is necessary to define each type. In Fig. 10, such definition is described schematically. The criteria are not always strictly defined, resulting in bringing about intermediate cases. To establish such criteria, it is better to define by using some definite numbers. For this purpose, the numbers for the integrated fractions for ^{40}Ar and ^{36}Ar (and ^{37}Ar) are used at the point of the integrated fraction of 0.5 for ^{39}Ar. The definitions are as follows (at $\Sigma Fi\ (^{39}Ar)=0.5$).

Type A: $\Sigma Fi\ (^{40}Ar)$, 0.5 ± 0.1,
$\Sigma Fi\ (^{36}Ar)$, $\Sigma Fi\ (^{37}Ar)\geq 0.2$.

Type B: $\Sigma Fi\ (^{40}Ar)$, 0.5 ± 0.1,
$\Sigma Fi\ (^{36}Ar)$, $\Sigma Fi\ (^{37}Ar)<0.2$.

Type C: $\Sigma Fi\ (^{40}Ar)$, <0.4 or >0.6
$\Sigma Fi\ (^{36}Ar)$, $\Sigma Fi\ (^{37}Ar)$—not always correlated.

Figures 7, 8 and 9 are considered to represent Types A, B and C, respectively.

Based on such criteria, the Antarctic meteorites whose ^{40}Ar-^{39}Ar ages were obtained previously (KANEOKA, 1980, 1981, 1983b; KANEOKA *et al.*, 1979) are classified into three types according to their Ar degassing patterns. Results are summarized in

Table 2. Summary of ^{40}Ar-^{39}Ar ages and degassing types of Antarctic meteorites.

Meteorite	Class	^{40}Ar-^{39}Ar Age* (Ma)		Degassing type**
		Plateau	Total	
Chondrite				
Y-74640	H5–6	4407	4317	B
ALH-77288,62	H6	4460	4759	B–C
63	H6	4497	4764	B–C
Y-74191	L3	—	3558	B–C
ALH-77015	L3	(4514)	4065	B
Y-74190	L6	357	443	B
ALH-761,61	L6	—	4431	B–C
62	L6	—	4579	B–C
64	L6	4487	4417	B
ALH-77214	L or LL	—	3105	C
ALH-77304	LL3	4503	3680	C
Y-75258	LL6	4377	4381	B
Achondrite				
Y-74159	Eucrite	4075	4043	A
Y-74450	Eucrite	4012	4045	A
ALH-765	Eucrite	(3438)	3251	A
Y-7308	Howardite	4480	4538	A–C
Y-74097	Diogenite	1100	1190	A–C

*Data sources for ^{40}Ar-^{39}Ar ages: KANEOKA (1980, 1981, 1983b), KANEOKA *et al.* (1979).
**Degassing types are defined in Fig. 10.

Table 2 together with ^{40}Ar-^{39}Ar age data. It is interesting to note that Type A is observed only among achondrites and Type B among chondrites, respectively. Type C is observed among both kinds of meteorites. However, there seems to be no correlation between the degree of equilibrium state of a chondrite and the degassing type

defined here. These results can be explained as follows.

By definition, meteorites with Type A or Type B show Ar-degassing patterns where ^{40}Ar correlates well with ^{39}Ar. This means that most radiogenic ^{40}Ar are located at K-sites in such meteorites, suggesting no great disturbance for obtaining meaningful ^{40}Ar-^{39}Ar ages. However, the disturbance here means that of non-thermal origin like the effect of weathering. Because highly shocked meteorites are included in Type A or Type B. The sample Y-74190 classified as Type B is a typical example which clearly indicates the occurrence of serious degassing of ^{40}Ar due to a later event such as collision of parent bodies. Relatively young ^{40}Ar-^{39}Ar ages are compatible with this interpretation (*e.g.* BOGARD *et al.*, 1976). Both eucrites Y-74159 and Y-74450 are classified into Type A and considered to have experienced a shock event (TAKEDA *et al.*, 1978). At the time of serious shock event, the energy produced by the collision would have raised the temperature, causing partial Ar loss from a meteorite. The present results suggest that the correlation between ^{40}Ar and ^{39}Ar is kept for these meteorites, because most of observed ^{40}Ar are considered to have been produced after the event. The difference between Type A and Type B resides in the fact that ^{36}Ar and ^{37}Ar degass at slightly higher temperatures than ^{39}Ar in Type A, but at much higher temperatures in Type B The apparent correlation between ^{36}Ar and neutron induced Ca-derived ^{37}Ar suggests that the observed ^{36}Ar is mostly trapped at similar sites with Ca, implying cosmogenic origin for ^{36}Ar. Hence, in Type A meteorites K and Ca are considered to be located at similar sites or phases, but at different phases in Type B meteorites. This mostly reflects the differences both in mineralogy and the distribution of grain sizes between chondrites and achondrites. In general, the components of ^{36}Ar comprise cosmogenic and trapped ones. In the present study, I discuss the mixed ones due to the lack of sufficient information to separate these components. Some uncertainties might be caused by different degree of mixing between cosmogenic and trapped components. As long as we discuss the general trend of degassing type of Ar, however, it does not change the classification from one type to the other.

It is worth noting that those meteorites which are classified into Type C mostly show the effect of weathering in their ^{40}Ar-^{39}Ar ages. For example, the samples ALH-77288,62 (H6) and ALH-77288,63 (H6) indicate the effect of atmospheric contamination as revealed in their high total ^{40}Ar-^{39}Ar ages together with anomalously high ^{40}Ar-^{39}Ar ages at the intermediate temperatures (KANEOKA, 1983a, b). Similar effects are observed for both ALH-761,61 (L6) and ALH-761,62 (L6) (KANEOKA, 1983a, b). The sample ALH-77214 (L or LL) is a seriously weathered one (KANEOKA, 1980). In the case of ALH-77304 (LL3), we have no evidence of thermal disturbance, whereas it loses a large amount of ^{40}Ar as revealed in its total ^{40}Ar-^{39}Ar age compared with plateau ^{40}Ar-^{39}Ar age. Hence it is inferred that much Ar loss probably occurred due to the effect of non-thermal event like weathering. The situation is quite similar for the sample Y-74191 (L3). In the cases of the samples Y-7308 (Ho) and Y-74097 (Di), the effect of weathering seems not so clear as long as their plateau and total ^{40}Ar-^{39}Ar ages in the lowest temperature fractions together with the unproportionally large rate of degassing of ^{36}Ar (KANEOKA, 1981; KANEOKA *et al.*, 1979). This suggests that they are also weathered to some extent. Thus, samples which are classified into Type C seem to have been more or less affected by non-thermal effects such as weathering.

Such effects on the obtained ^{40}Ar-^{39}Ar ages differ for each meteorite. Hence if we observe such Ar-degassing pattern as classified into Type C, we should be very careful in interpreting the obtained ^{40}Ar-^{39}Ar age for the meteorite. Thus, such classification of Ar-degassing would give us another measure to evaluate the reliability of an ^{40}Ar-^{39}Ar age obtained for an Antarctic meteorite.

The classification would not sufficiently be defined at present, because many samples should have been classified as intermediate between the two types. Even in this case, however, when we observe a sample classified into Type C or intermediate between the Type C and the other type, such information would be of great help for evaluating the reliability of the obtained ^{40}Ar-^{39}Ar ages.

Acknowledgments

I would like to appreciate Prof. T. NAGATA and Dr. K. YANAI of the National Institute of Polar Research for providing the Antarctic meteorite samples. This study was financially supported in part by the Ministry of Education, Science and Culture.

References

BOGARD, D. D., HUSAIN, L. and WRIGHT, R. J. (1976): ^{40}Ar-^{39}Ar dating of collisional events in chondritic parent bodies. J. Geophys. Res., **81**, 5664–5678.

FECHTIG, H. and KALBITZER, S. (1966): The diffusion of argon in potassium-bearing solids. Potassium Argon Dating, comp. by O. A. SCHAEFFER and J. ZÄHRINGER. Berlin, Springer, 68–107.

KANEOKA, I. (1980): ^{40}Ar-^{39}Ar ages of L and LL chondrites from Allan Hills, Antarctica; ALHA-77015, 77241 and 77304. Mem. Natl Inst. Polar Res., Spec. Issue, **17**, 177–188.

KANEOKA, I. (1981): ^{40}Ar-^{39}Ar ages of Antarctic meteorites; Y-74191, Y-75258, Y-7308, Y-74450 and ALH-765. Mem. Natl Inst. Polar Res., Spec. Issue, **20**, 250–263.

KANEOKA, I. (1983a): Anomalously old ^{40}Ar-^{39}Ar ages of Antarctic meteorites due to weathering. Nature, **304**, 146–148.

KANEOKA, I. (1983b): Investigation of the weathering effect on the ^{40}Ar-^{39}Ar ages of Antarctic meteorites. Mem. Natl Inst. Polar Res., Spec. Issue, **30**, 259–274.

KANEOKA, I., OZIMA, M. and YANAGISAWA, M. (1979): ^{40}Ar-^{39}Ar age studies of four Yamato-74 meteorites. Mem. Natl Inst. Polar Res., Spec. Issue, **12**, 186–206.

TAKEDA, H., MIYAMOTO, M., YANAI, K. and HARAMURA, H. (1978): A preliminary mineralogical examination of the Yamato-74 achondrites. Mem. Natl Inst. Polar Res., Spec. Issue, **8**, 170–184.

VAN SCHMUS, W. R. and WOOD, J. A. (1967): A chemical-petrologic classification for the chondritic meteorites. Geochim. Cosmochim. Acta, **31**, 747–765.

(Received June 13, Revised manuscript received August 29, 1984)